

EFFECT OF ABLATION ENVIRONMENT ON THE CHARACTERISTICS OF GRAPHENE NANOSHEETS PRODUCED BY LASER ABLATION

ELNAZ VAGHRI^a, DAVOUD DORRANIAN^{a,*}

ABSTRACT. The effect of ablation environment on the characteristics of graphene sheets produced by the laser ablation method in liquid medium has been studied experimentally and reported here. Graphene sheets were synthesized by using Q-switch Nd-YAG laser at 532 nm wavelength and 7 ns pulse width and laser fluence of 0.5 J/cm² in liquid nitrogen and distilled water environments. The structure and morphology of the ablation products are characterized by X-ray diffraction method, UV-Visible absorption spectroscopy, transmission electron microscopy (TEM), Raman and Fourier transform infrared spectroscopy (FTIR). Results indicate that the graphene nanosheets synthesized by the laser ablation method in liquid nitrogen environment have larger sp² carbon domains and minor structural defects. Therefore, in our experimental conditions, the liquid nitrogen environment seems to be a better medium for producing graphene sheets with high quality, in comparison with the water.

Keywords: Pulsed laser ablation, Graphene, Carbon nanostructures, liquid nitrogen, TEM

INTRODUCTION

Carbon based nano-materials have been extensively studied in the last few decades. Among them graphene, which is a two-dimensional (2D) material with an in-plane hexagonal structure, has attracted more scientific interest, owing to its unprecedented and unique electrical, mechanical, and thermal properties [1,2]. Graphene and graphene based compounds found wide applications in different industrial fields such as electro-photoluminescence devices [3], solar cells [4], artificial muscles [5], beam-scanning planar lens [6], chemical sensors [7], biosensors [8] or organic light emitting diodes [9]. Due to their widespread applications, a large scale production of these materials is needed.

^a Laser Lab., Plasma Physics Research Center, Science and Research Branch, Islamic Azad University, Tehran, Iran

* Corresponding author: doran@srbiau.ac.ir

To develop the fabrication methods of graphene and its derivatives, many researches have been performed. Currently, numerous techniques are being tested to synthesize graphene such as chemicals vapor deposition, micromechanical exfoliation, epitaxial growth, electric arc graphene production, but among them, pulsed laser ablation (PLA) of a solid target in a confining liquid is emerged as a simple and most efficient technique for synthesizing various kinds of graphene nanoparticles and nanostructures. Laser wavelength, fluency, and pulse duration, as well as the liquid ablation environment and its temperature are the main parameters which could affect on the final production of the laser ablation process [10,11]. Ablation environment can affect the ablation products in two ways. Firstly, the liquid medium in laser ablation process can control the pressure of the plasma plume on the surface of the target, pressure directly proportional to the ablation liquid density; it can change the structure, size, and morphology of the produced nano-structures. Secondly, the aggregation of products can be affected by the nature of liquid environment like polarity or dispersion [10, 11]. During the interaction between the laser beam and the target, the plasma plume, consisting of vaporized atoms or molecules, ablated from the surface of the target, results due to extreme heating; in such conditions, atoms or molecules aggregate together to form nanoparticles. Subsequently, by increasing the pressure of plasma, the number of nanoparticles will also increase. On the other hand, decreasing the plasma pressure (and because of weak Van der Waals bonds between the graphite planes) gives rise to ablation products in the form of graphene planes [10]. The smaller density of the nitrogen in comparison with water and other appropriate liquids, makes this cryogenic a suitable medium for producing graphene nanosheets [10].

Graphene production in liquid nitrogen and distilled water different environments have been recently reported. Mortazavi and co-workers produced graphene sheets by using nanosecond Q-switched Nd:YAG laser ablation of a graphite target in the liquid nitrogen environments [12]. They explained the formation of the laser-ablated produced graphene sheets in liquid nitrogen by the penetration of liquid into the interlayer spacing of graphite. Sadeghi et al. synthesized carbon nanostructures in different liquid environments including distilled water, acetone, alcohol, and CTAB environments by using a 7 ns fundamental wavelength of pulsed Nd:YAG laser at 1064 nm [13]. Their results show that the highest amount of graphene sheets are produced in distilled water environment. Solati and co-workers used nanosecond pulsed laser ablation technique to fabricate colloidal ZnO nanoparticle and graphene nano composite in water environment [14]. Their results show that by increasing the amount of graphene in the suspensions, the band gap energy of mixtures was decreased noticeably. The purpose of the present experimental research is to investigate the effects of the ablation environment on the characteristics of carbon nanostructures produced by the laser ablation technique. In this respect, two different liquid environments: distilled water and liquid nitrogen have been tested.

RESULTS AND DISCUSSION

Raman spectroscopy is a useful and non-destructive diagnostic tool for distinguishing carbonaceous materials. The Raman spectra of the graphene suspensions are illustrated in Fig.1. Output data have been recorded from dried drops of both suspensions on glass substrates. The most prominent peaks in the Raman spectra of graphitic carbon based materials especially graphene are G, D and 2D bands. The G peak is related to plane stretching vibration mode of any pair of SP² bonded carbon atoms [15, 16]. The D band is arising from structural defects, edge effects and dangling SP² carbon bonds that break the symmetry on the hexagonal SP² bonded lattices [17]. The peak at a wave number of 1192 cm⁻¹ (named as D* peak) is caused by wrinkled (defective) morphology of the graphene sheets [18]. In Fig. 1(a) two individual peaks at around 1384 cm⁻¹ and 1545 cm⁻¹ are related to the D and G bands, respectively. Furthermore, another disorder induce-peak which is named as D_r peak at the wave number of 1612 cm⁻¹ can be seen in this spectrum. The D_r peak is resulted from intra-valley double-resonance process [19]. As shown in Fig.1 (b) the D peak for the graphene samples produced in distilled water is observed at the same wave number of 1384 cm⁻¹ with larger intensity, while the G peak shift to higher wave number at 1633 cm⁻¹ and becomes broadens.

The main peaks in the Raman spectra of carbons are the so-called G and D bands, usually appearing at 1560 and 1360 cm⁻¹ respectively. The G band has a shift about 73 cm⁻¹ to higher wave numbers, due to the conjugation of alkenic C=C bonds with the C=C bonds in aromatic rings (usually longer than those in unconjugated alkenic sp² sites), as reported by Kimiagar et al. [20]. Furthermore, there are other additional peaks at approximately 2950 cm⁻¹ and 2965 cm⁻¹ in the Raman spectra of the samples produced in the distilled water and liquid nitrogen environments, respectively. These peaks are originating from the combination of the D and G bands, called as D+G band [21]. It is worth noting that the intensity of the disorder-induced D band for the graphene sheets produced in liquid nitrogen environment is smaller than for the product in water, indicating the improved quality of graphene nanosheets in liquid nitrogen. The intensity ratio of the disorder-induced D band to the G band (I_D/I_G) is inversely proportional to the in-plane graphitic crystallite size, as given by the formula [22-24]: $L_a = 4.4 (I_G/I_D)$.

The calculated results show that the I_D/I_G ratio for the graphene sheets produced in liquid nitrogen environment (0.25) is smaller than this ratio in distilled water environment (0.94), indicating that the sp² domain of the graphene sheets produced in liquid nitrogen (17.6 nm) is larger than for the product in distilled water environment (4.6 nm). Besides, we can see prominent peaks at the wave numbers of 2688 cm⁻¹ and 2757 cm⁻¹ in the Raman spectra of the samples produced in liquid nitrogen and distilled water environments, respectively. These peaks are the characteristic peaks of the graphene structure, arising from

a two-phonon double resonance Raman scattering process [25]. The increase of the intensity of 2D band for the graphene nanosheets produced in liquid nitrogen environment indicates that number of layers in the sample produced in liquid nitrogen is smaller than for the product obtained in water [26].

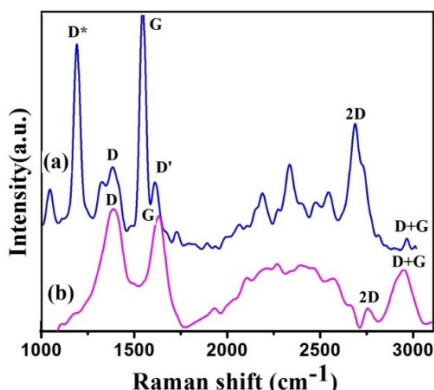


Figure 1. Raman spectra of the samples produced by pulsed laser ablation in (a) liquid nitrogen and (b) distilled water environments

The optical spectra of the samples with the transmittance of the liquid environment as the baseline are indicated in Fig. 2. The transmittance spectra of the samples produced in liquid nitrogen environment indicate a high transparency (99%) while the transparency is decreased in the sample produce in distilled water (96%). It is an evidence that the graphene nanosheets produced in distilled water become thicker. This result is in good agreement with the result of the Raman spectra.

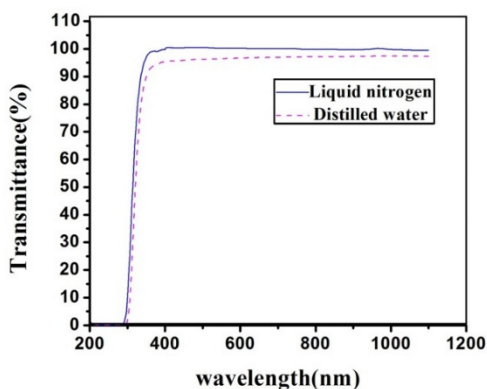


Figure 2. Optical transmittance spectra of the graphene nanosheets Produced in liquid nitrogen and distilled water environments

The TEM micrographs of the samples are shown in Fig. 3. Data have been recorded from the dried drops of suspensions on carbon coated copper grids. The images show the transparent silk like structures of graphene. More Darkness in the images is referred to the regions that several graphene layers are stacked on each other. According to the experimental observations, the graphene sheets produced in liquid nitrogen medium have smaller number of layers in compared to those produced in distilled water environment.

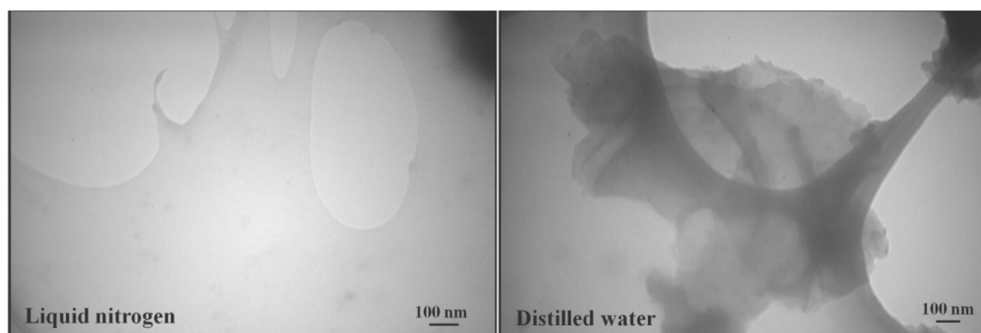


Figure 3. TEM micrographs of the samples

The X-ray diffraction patterns of the samples are presented in Fig. 4. XRD measurement is carried out using the dried drops of every suspension on Si substrates. The XRD pattern of the sample produced in liquid nitrogen environment shows two prominent reflection peaks. The reflection peak at $2\theta=32.1^\circ$ is related to graphitic carbon in graphene while that at $2\theta=69.6^\circ$ corresponds to the Si substrate. One can see a sharp peak at $2\theta=69.5^\circ$ attributed to Si substrate in the XRD pattern of the samples produced in distilled water. The disappearance of graphene peak in XRD diffraction pattern of the product in distilled water may be due to small number of graphene planes resulted in this environment. Basically the peaks in XRD diffraction pattern of materials are the reflected X-ray photons from the atoms on the successive planes of their lattice, which satisfy the Bragg's condition. When the number of planes is small, one may not expect large reflection of X-ray photons [14].

The FTIR transmitted spectra of the studied samples recorded in the range of $500\text{-}4000\text{ cm}^{-1}$ are shown in Fig.5. In the low frequency area, there are absorption peaks at the wave numbers of 700 and 732.17 cm^{-1} originating from vibrations of C-H bonds [10]. The aromatic C=C vibrations cause the appearance of a peak at around 1640 cm^{-1} [27]. Beside, the peaks which are located at around 2078.41 cm^{-1} , 2082.7 cm^{-1} can be due to $\text{sp}^2\text{ C=C}$ groups.

Furthermore, in the high frequency area, the presence of broad absorption band in the range of $3100\text{-}3700\text{ cm}^{-1}$ arises from the stretching vibrations of O-H groups. As shown in Fig.5 the intensity of absorption peaks in the samples is similar. The intensity of the absorption peaks in the FTIR spectra depends on the number of the specific bonds present in the samples [10].

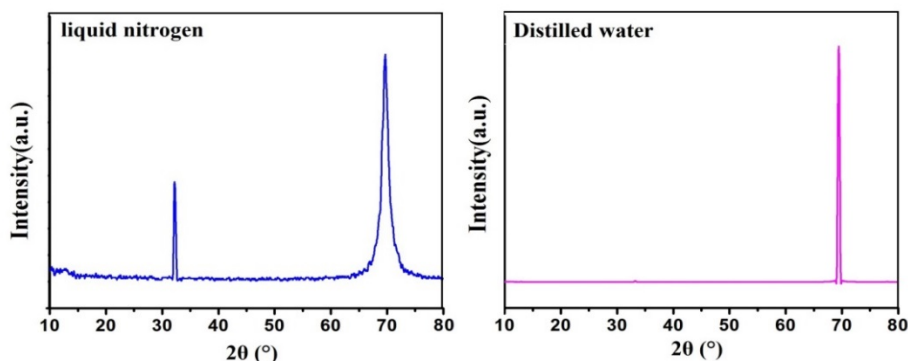


Figure 4. X-ray diffraction pattern of the samples produced by pulsed laser ablation

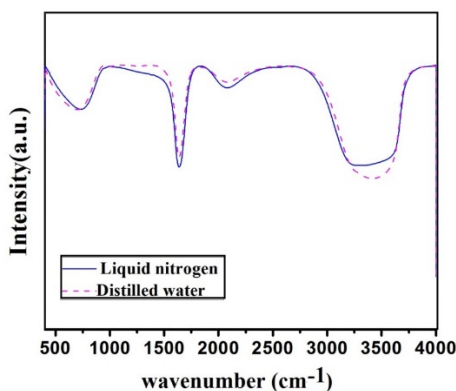


Figure 5. FTIR spectra of the samples

CONCLUSIONS

Graphene sheets were prepared using the second harmonic of a Nd:YAG laser operating at 532 nm wavelength. In this study, the effect of laser ablation environment on the characteristics of the produced graphene sheets

has been investigated. The Raman spectra indicate that the graphene sheets produced in liquid nitrogen environment have larger sp^2 carbon domains, lower structural defects and consequently more acceptable quality compared to the samples produced in distilled water. The X-ray diffraction pattern indicates a smaller number of graphene planes formed in distilled water environment. The TEM micrographs indicate the formation of silk-like structure in the samples. The optical transmittance spectra show the thicker graphene nanosheets are formed in distilled water environment. The FTIR results revealed the existence of sp^2 C=C groups in the graphene nanosheets in suspensions. Corroborating the experimental data, it appears that the liquid nitrogen is a more suitable medium for producing graphene nanosheets with laser ablation method in comparison with the water and other appropriate liquids.

EXPERIMENTAL SECTION

Graphene sheets are prepared by pulsed laser ablation of a high purity graphite target (with 99.99% purity) using the second harmonic of a Nd:YAG laser at a wavelength of 532 nm, with 7 ns pulse width and pulse-repetition rate of 5 Hz and a pulse fluency of 0.5 J/cm^2 at the room temperature. Before starting the experiments, both targets and containers were cleaned ultrasonically in ethanol, acetone and distilled water solutions respectively for 15 minutes. Graphite target was placed at the bottom of a glass cylindrical vessel containing liquid. Height of liquid on the target was 0.8 cm. The laser beam with 6 mm in diameter was focused on the target surface using a lens with a focal length of 80 mm. In order to study the effects of ablation environment on the production quality of Graphene sheets the samples were prepared in distilled water and liquid nitrogen environments. In this study, various analytical techniques have been used to characterize the structure of produced samples. IR spectrum of samples (FTIR), were Cary out using NEXUS870 FTIR spectrometer from Thermo Nicolet Co., in the range of $500\text{-}4000 \text{ cm}^{-1}$. Optical transmittance spectra of the samples were measured by UV-Vis-NIR spectrophotometer from PG Instruments (T-80). X-ray diffractions of the dried graphene suspensions on silicon substrates are analyzed using a Cu-K α radiation ($\lambda=1.54060\text{\AA}$) diffractometer. Raman measurements are performed employing an Almega Thermo Nicolet Dispersive Raman Spectrometer with a 532 nm Nd:YLF laser. Transmission electron microscopy micrographs were taken using a Zeiss-EM10C microscope.

REFERENCES

- [1]. M.J. Allen, V.C. Tung, and R.B. Kaner, *Chem. Rev.*, **2009**, *110*, 132-145.
- [2]. Y. LI, N. CHOPRA, the Minerals, *Chemical Methods*, **2015**, *67*(1), 34.
- [3]. Z.T. Luo, P.M. Vora, E.J. Mele, A.T.C. Johnson, J.M. Kikkawa, *Appl. Phys. Lett.* **2009**, *94*, 111909.
- [4]. H.S. Park, J.A. Rowehl, K.K. Kim, V. Bulovic, and J. Kong, *Nanotechnology* **2010**, *21*, 505204.
- [5]. J.J. Liang, Y. Huang, J.Y. Oh, M. Kozlov, D. Sui, S.L. Fang, R.H. Baughman, Y.F. Ma, Y.S. Chen, *Adv. Funct. Mater.*, **2011**, *21*, 3778-3784.
- [6]. H.J. Xu, W.B. Lu, Y. Jiang, and Z.G. Dong, *Appl. Phys. Lett.*, **2012**, *100*, 051903.
- [7]. A. Salehi-Khojin, D. Estrada, K.Y. Lin, K. Ran, R.T. Haasch, J.-M. Zuo, E. Pop, and R.I. Masel, *Appl. Phys. Lett.*, **2012**, *100*, 033111.
- [8]. B. Song, G. Cuniberti, S. Sanvito, and H.P. Fang, *Appl. Phys. Lett.*, **2012**, *100*, 063101/1-4.
- [9]. J.B. Wu, M. Agrawal, H.A. Becerril, Z.A. Bao, Z.F. Liu, Y.S. Chen, P. Peumans, *ACS Nano*, **2010**, *4*, 43.
- [10]. N. Tabatabaie, D. Dorrnian, *Appl. Phys. A*, **2016**, *122*, 558.
- [11]. M. Morad, E. Solati, S. Darvishi, D. Dorrnian, *Cluster Sci.*, **2016**, *27*, 127.
- [12]. Z. Mortazavi, P. Parvin, A. Reyhani, *Laser Phys. Lett.*, **2012**, *9*, 547.
- [13]. H. Sadeghi, D. Dorrnian, *Theor Appl Phys*, **2016**, *10*, 7.
- [14]. E. Solati, D. Dorrnian, *Appl. Phys. B*, **2016**, *122*, 76.
- [15]. J. Ding, M. Wang, X. Zhang, Z. Yang, X. Song, Ch. Ran, *SCI*, **2014**, *416*, 289.
- [16]. C. Casiraghi, *Phys. Rev. B*, **2009**, *80*, 233407.
- [17]. A. Aregahegn Dubale., Su Wei-Nien, A. G. Tamirat, Ch.J. Pan, B. A. Aragaw, H-M.-Chen, Ch-H Chen, B.J. Hwang, *Mater. Chem. A*, **2014**, *2*, 18383.
- [18]. A. Kaniyoor, S. Ramaprabhu, *AIP Advances*, **2012**, *2*, 032183.
- [19]. J. Jiang, R. Pachter, F. Mehmood, A.E. Islam, B. Maruyama, J.J. Boeck, A, *carbon*, **2015**, *90*, 53.
- [20]. S. Kimiagar, N. Rashidi, *Advanced Research*, **2015**, *3*, 153.
- [21]. Y. Kawashima, G. Katagiri, *Physical Review B*, **1995**, *52*, 10053.
- [22]. T.V. Cuong, V.H. Pham, E.W. Shin, J.S. Chung, S.H. Hur, E. J. Kim, Q.T. Tran, H.H. Nguyen, P.A. Kohl, *Applied Physics Letters*, **2011**, *99*, 041905.
- [23]. M. Shafiei, P.G. Spizzirri, R. Arsat, J. Yu, J.D. Plessis, S. Dubin, R.B. Kaner, K. Kalantar-zadeh, and W. Wlodarski, *J. Phys. Chem. C*, **2010**, *114*, 13796.
- [24]. A.C. Ferrari, *Solid State Commun.*, **2007**, *143*, 47.
- [25]. R.J. Sereshta, M. Jahanshahia, A. Rashidi, A.A. Ghoreyshia, *APPL SURF SCI*, **2013**, *276*, 672.
- [26]. S. Berciaud, S. Ryu, L.E. Brus, T.F. Heinz, *Nano Lett.*, **2009**, *9*, 346.
- [27]. O. Akyildirim, H. Medetalibeyoğlu, S. Manap, M. Beytur, FS. Tokalı, ML. Yola, N. Atar, *Electro.chem. Sci.*, **2015**, *10*, 7743.